



ELSEVIER

Journal of Non-Crystalline Solids 299–302 (2002) 1321–1325

JOURNAL OF
NON-CRYSTALLINE SOLIDS

www.elsevier.com/locate/jnoncrsol

Characterization and control of defect states of polycrystalline silicon thin film transistor fabricated by laser crystallization

H. Watakabe ^{*}, Y. Tsunoda, N. Andoh, T. Sameshima

Faculty of Technology, Tokyo University of Agriculture and Technology, Tokyo 184-8588, Japan

Abstract

Improvement of characteristics of polycrystalline silicon thin film transistors (poly-Si TFTs) was achieved by defect reduction methods of oxygen plasma at 250 °C and at 30 W and 1.25×10^6 -Pa high-pressure H₂O vapor heat treatments at 270 °C. Numerical analysis of transfer characteristics revealed that the combination of oxygen plasma for 40 min with the high-pressure H₂O vapor annealing for 3 h effectively reduced the densities of deep level states from 1.4×10^{18} (as crystallized) to 1.6×10^{17} cm⁻³ and the densities of tail states from 9.2×10^{18} (as crystallized) to 2.7×10^{18} cm⁻³, respectively. The threshold voltage of transfer characteristics was reduced from 4.1 to 1.3 V through the defect reduction. © 2002 Published by Elsevier Science B.V.

PACS: 61.50.-b; 71.20.-b; 73.40.Qr; 85.30.Tv

1. Introduction

Reduction of defects in polycrystalline silicon (poly-Si) films at low temperatures is very important for fabrication of electronic devices such as thin film transistors (TFTs) and solar cells [1–6]. We have reported simple heat treatment with oxygen plasma or high-pressure H₂O vapor for defect reduction [7–9]. Improvements of electrical properties of SiO₂ films, SiO₂/Si interfaces and poly-Si films have been achieved by the those methods. In this paper, we discuss improvements of characteristics of poly-Si TFTs using defect reduction methods of heat treatment with oxygen plasma or

high-pressure H₂O vapor. Numerical analysis of the transfer characteristics gives the change in distribution of the density of defect states. The relation of the threshold voltage between the densities of defect states and positive fixed oxide charges is reported. The carrier mobility of poly-Si TFTs is also discussed.

2. Experimental

N-channel-Ta-top-gate-type poly-Si TFTs were fabricated. Amorphous silicon films with a thickness of 50 nm were formed by low-pressure-chemical-vapor deposition (LPCVD) on quartz substrates. The samples were placed in a chamber, which was evacuated by a turbo molecular pump to a level of 1×10^{-4} Pa. Crystallization of the

^{*} Corresponding author.

E-mail address: watakabe@cc.tuat.ac.jp (H. Watakabe).

silicon films was carried out at 250 °C by irradiation of 28-ns pulsed XeCl excimer laser. The laser energy density was increased from 160 to 440 mJ/cm² in 20 mJ/cm² steps. Twenty pulses were irradiated at each laser energy density. Immediately after laser crystallization, oxygen plasma treatment at 250 °C at 130 Pa for 40 min was carried out with a rf power of 30 W for reduction of defect density in polycrystalline silicon films [7]. Hundred-nm thick SiO₂ films were deposited as gate insulator at 200 °C using electron-cyclotron resonance PECVD. Source and drain regions were formed by phosphorus-ion implantation self-aligned with Ta gate electrodes. Activation of the dopant atoms were carried out by heating sample at 300 °C for 5 h. After fabrication of the TFT structure with a gate width of 10 μm and a length of 10 μm, heat treatment with high-pressure H₂O vapor was conducted. Samples and pure water were placed into the pressure-proof stainless-steel chamber. The chamber was heated at 270 °C for 3 h. H₂O was evaporated during heating and the pressure in the chamber was increased to 1.3 × 10⁶ Pa [8,9].

3. Results

Fig. 1 shows transfer characteristics of TFTs fabricated using laser crystallization at 440 mJ/cm² with 20 shots. The TFT fabricated with no oxygen plasma or no H₂O vapor heat treatment showed low drain currents with a carrier mobility of 92 cm²/V s and a high threshold voltage of 4.1 V. The TFT fabricated with oxygen plasma showed high drain current with a high carrier mobility of 138 cm²/V s and a low threshold voltage of 3.2 V. The mobility and threshold voltage were also improved to 103 cm²/V s and 2.9 V, respectively, by 1.25 × 10⁶-Pa H₂O vapor annealing at 270 °C for 3 h after fabrication of TFT structure. Both treatments with oxygen plasma and high-pressure H₂O vapor marked improved transfer characteristics as shown in Fig. 1. The carrier mobility was 153 cm²/V s. The threshold voltage decreased to 1.3 V.

Transfer characteristics were analyzed using a numerical calculation program developed with

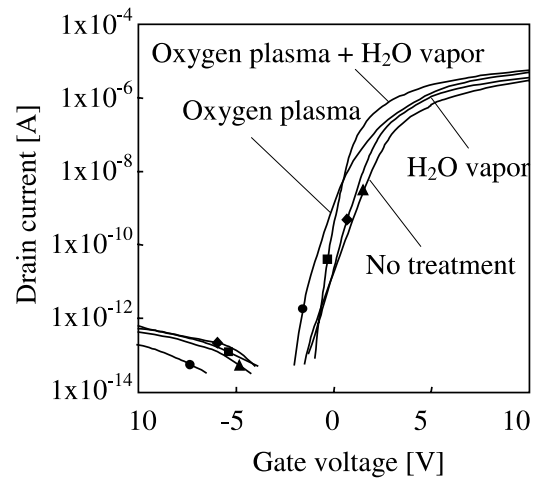


Fig. 1. Transfer characteristics of the TFTs fabricated with no oxygen plasma or no high-pressure H₂O vapor heating, only with oxygen plasma, only with H₂O vapor annealing and with oxygen plasma followed by high-pressure H₂O vapor annealing. Oxygen plasma treatment was carried out at 250 °C for 40 min. The H₂O vapor annealing was conducted at 270 °C and 1.25 × 10⁶ Pa for 3 h. Laser crystallization was carried out at 440 mJ/cm² and 20 shots. The drain voltage was 0.1 V. The ratio of channel width to channel length was 1.

finite-element method combined with statistical thermodynamical conditions with defect states localized at SiO₂/Si interfaces as well as silicon films. The deep-level defect states localized at the mid gap were introduced. A Gaussian-type energy distribution was assumed. The peak density located at the mid gap. The width of the deep level states was defined as the distance between the energies at which the density was e^{-1} × the maximum density. Tail-state-type defect states were also introduced. The density exponentially decreased from the conduction band edge to deep energy level in the band gap. The maximum density at the band edge of the tail states was assumed to be 2.8 × 10¹⁹ cm⁻³ eV⁻¹. The energy width of the tail states was determined as energy at which the density of the tail states was e^{-1} × the maximum density. The defect states were placed at SiO₂/Si interfaces as well as in silicon films. The density of positive fixed oxide charge was also introduced in the SiO₂ gate insulator just adjacent the gate electrode. The Fermi level in the channel region was determined under the charge neutrality

condition among the density of charge accumulated at the gate electrode due to gate voltage application, the density of fixed oxide charge, the density of charged defect states, impurity-ion concentration and the densities of free carriers among the gate electrode, the gate oxide and silicon channel regions. The Fermi–Dirac distribution function determined the carrier density and the occupied probability of defect states. The carrier mobility was also calculated with effects of impurity scattering and lattice scattering depending on the electrical field caused by gate voltage application. The distribution of the density of defect states, the carrier density and the carrier mobility were obtained through fitting of calculated transfer characteristics to experimental characteristics from low drain current regions in the subthreshold region to high current region above the threshold voltage, as shown in Fig. 1.

Fig. 2 shows the distribution of defect density in the energy band gap. Silicon films in the channel region had a high density of defect states for crystallization at 440 mJ/cm^2 and 20 shots in the case of no oxygen plasma or no H_2O vapor heat treatment. The tail states had a width of 0.16 eV and the density of $9.2 \times 10^{18} \text{ cm}^{-3}$. The deep level states localized at the mid gap had a peak density of $4 \times 10^{18} \text{ cm}^{-3} \text{ eV}^{-1}$ and a volume density of

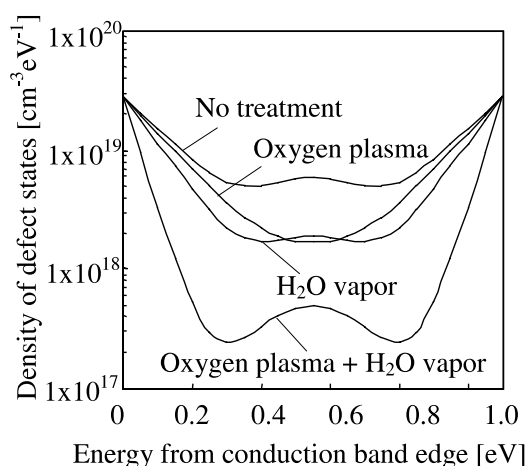


Fig. 2. Distribution of defect density in the band gap obtained by analysis of transfer characteristics in the cases of different defect reduction process steps.

$1.4 \times 10^{18} \text{ cm}^{-3}$. Oxygen plasma treatment just after crystallization effectively reduced the peak density and the volume density of the deep defect states to $5 \times 10^{17} \text{ cm}^{-3} \text{ eV}^{-1}$ and to $1.8 \times 10^{17} \text{ cm}^{-3}$. It also reduced the density of tail states to $8.1 \times 10^{18} \text{ cm}^{-3}$. On the other hand, the numerical analysis revealed that heat treatment at $270 \text{ }^\circ\text{C}$ for 3 h with $1.25 \times 10^6 \text{ Pa-H}_2\text{O}$ vapor reduced the density of tail states to $6.4 \times 10^{18} \text{ cm}^{-3}$, although there was a residual defect states at deep level with a volume density of $5.3 \times 10^{17} \text{ cm}^{-3}$. H_2O vapor was effective to reduce the density of defect states after TFT fabrication. Although there were multiple layers of gate insulator and gate metal overlaying the silicon layer, H_2O vapor effectively incorporated into the silicon films through the layers and made the defect states electrically inactive. The combination of the two heat treatments of oxygen plasma and H_2O vapor effectively reduced the densities of tail states and deep level states to 2.7×10^{18} and $1.6 \times 10^{17} \text{ cm}^{-3}$, as shown in Fig. 2.

Fig. 3 shows the threshold voltage as a function of the total density of the defect states. The experimental threshold voltage obtained from the linear relation between the drain current and the gate voltage was high at 4.1 V when the total

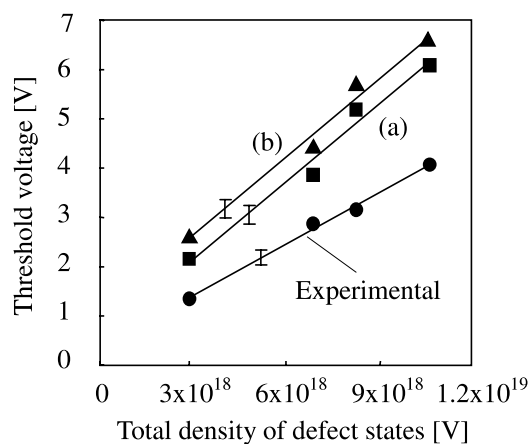


Fig. 3. Changes in the experimental threshold voltage, subtracted positive fixed oxide charge effect (a) and theoretical threshold voltage (b), which is subtracted fixed oxide charge effect and difference of work function between gate metal and silicon layer.

density of defect states was $1.1 \times 10^{19} \text{ cm}^{-3}$. The threshold voltage decreased as the density of defect states was reduced by oxygen plasma and high-pressure H_2O vapor annealing. The combination of oxygen plasma and high-pressure H_2O vapor annealing reduced the total density of defect states to $2.9 \times 10^{18} \text{ cm}^{-3}$. The threshold voltage was 1.3 V. High-pressure H_2O vapor annealing reduced the density of defect states in the SiO_2 gate insulator as well as silicon films. Analysis of our numerical calculation program revealed that the density of positive fixed oxide charge was reduced from 3×10^{11} to $1.5 \times 10^{11} \text{ cm}^{-2}$. The positive fixed oxide charge generates an internal electrical field at silicon and makes transfer characteristics shift to the negative gate voltage direction. When this threshold voltage reduction effect due to the fixed oxide charge was removed, the threshold voltage became higher as shown by the line (a) in Fig. 3. The difference of work function between Ta gate metal and silicon was -0.49 V . It is another reduction effect for the threshold voltage. The line (b) in Fig. 3 $(C_{\text{ox}}V_dW/L)^{-1}\partial I_d/\partial V_g$ is the calculated threshold voltage with no reduction effect due to fixed oxide charge or no difference of work function. The high defect density resulted in a high calculated-threshold voltage of 6.6 V in the case of no oxygen plasma or no high-pressure H_2O vapor

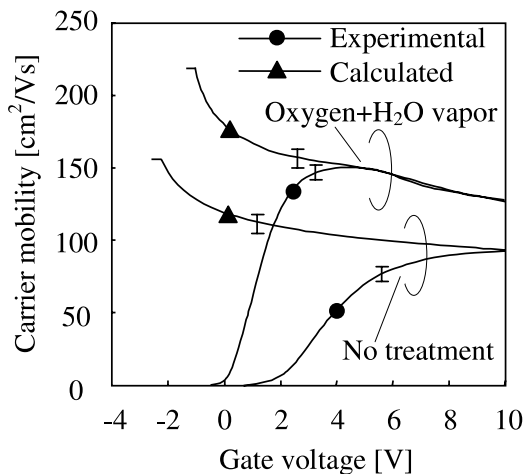


Fig. 4. Experimental and calculated carrier mobility as a function of gate voltage of the TFTs with no defect reduction treatment and combination of oxygen plasma treatment and high-pressure H_2O vapor heat treatment.

annealing. A high gate voltage is necessary for operating TFTs with a high defect density. A low calculated-threshold voltage of 2.6 V was achieved with the combination of oxygen plasma and high-pressure H_2O vapor annealing.

Fig. 4 shows the calculated and experimental effective carrier mobility as a function of the gate voltage for TFTs fabricated with no defect reduction treatment and with the oxygen plasma combined with high-pressure H_2O vapor annealing. The experimental effective mobility was obtained from the simple linear equation of the drain current with the gate voltage of $(C_{\text{ox}}V_dW/L)^{-1}\partial I_d/\partial V_g$. The experimental effective mobility was very low at the low gate voltage region especially for TFT with no defect reduction treatment.

4. Discussion

Defect reduction methods of oxygen plasma treatment and high-pressure H_2O vapor heat treatment improve transfer characteristics as shown in Fig. 1; the threshold voltage decreased to 1.3 V and the effective carrier mobility increased to $153 \text{ cm}^2/\text{Vs}$ for combination of oxygen plasma after laser crystallization with high-pressure H_2O vapor heat treatment after fabrication of TFT structure. Analysis of transfer characteristics using a numerical calculation program revealed that the densities of tail states and deep level states in silicon films were effectively reduced to 2.7×10^{18} and $1.6 \times 10^{17} \text{ cm}^{-3}$ by the combination of oxygen plasma with high-pressure H_2O heat treatment. The present analysis also revealed that the threshold voltage was governed by the density of defect states. There was the high density of tail states of $9.2 \times 10^{18} \text{ cm}^{-3}$ in poly-Si TFT fabricated by laser crystallization. The high density of defect states caused a high threshold voltage of 6.6 V. The threshold voltage was effectively reduced to 2.3 V through the reduction of the density of defect states by oxygen plasma and high-pressure H_2O vapor heat treatment.

Moreover, defect states also reduced the effective carrier mobility. The effective carrier density was low at the low gate voltage region compared with the density of accumulated charge, because

the charge neutrality completed between positive charges at gate electrode and defect states negatively charged in silicon when there was a high density of defect states especially tail states. Fermi level did not move to the conduction band edge because of charging the defect states with the low gate voltage condition. The reduction of the density of defect states allowed a high mobility at the low gate voltage region as shown in Fig. 4. A high gate voltage caused a high electrical field so that the carrier mobility decreased as the gate voltage increased as shown by curves of calculated mobility. Reduction of the experimental effective mobility in the high gate voltage region was caused by increase of phonon scattering probability due to narrowing the channel depth associated with a high electrical field. The high defect density can cause a high electrical field at channel region because the high density of charged defect states results in band bending in silicon. Reduction of defect states makes it possible to operate TFTs with a low electrical field with a high mobility.

5. Summary

We discussed defect reduction behaviors of polycrystalline silicon thin film transistors (poly-Si TFTs) using oxygen plasma and high-pressure H₂O vapor heat treatments. A finite element numerical analysis program combined with statistical thermodynamical conditions was developed to analyze the distribution of the density of defect states in the band gap for the channel region. Oxygen plasma treatment at 270 °C and 30 W for 40 min just after XeCl laser crystallization effectively reduced the density of defect states at deep energy level from 1.4×10^{18} (as fabricated) to

$1.8 \times 10^{17} \text{ cm}^{-3}$. Heat treatment at 270 °C for 3 h with $1.25 \times 10^6 \text{ Pa-H}_2\text{O}$ vapor reduced the density of tail states from 9.2×10^{18} (as fabricated) to $6.4 \times 10^{18} \text{ cm}^{-3}$. Improvement of characteristics of poly-Si TFTs was achieved by the combination of oxygen plasma treatment and high-pressure H₂O vapor annealing. The total density of defect states were reduced from 1.1×10^{19} (as fabricated) to $2.9 \times 10^{18} \text{ cm}^{-3}$. The threshold voltage of transfer characteristics was reduced from 4.1 to 1.3 V through the defect reduction. The reduction of defect states resulted in a high effective carrier mobility of $153 \text{ cm}^2/\text{V s}$ because of low gate voltage operation and the high carrier density.

Acknowledgements

We thank Dr S. Higashi, Dr T. Mohri and Professor T. Saitoh for their support.

References

- [1] T. Sameshima, S. Usui, M. Sekiya, IEEE Electron Device Lett. 7 (1986) 276.
- [2] K. Sera, F. Okumura, H. Uchida, S. Itoh, S. Kaneko, K. Hotta, IEEE Trans. Electron Devices 36 (1989) 2868.
- [3] T. Serikawa, S. Shirai, A. Okamoto, S. Suyama, Jpn. J. Appl. Phys. 28 (1989) L1871.
- [4] A. Kohno, T. Sameshima, N. Sano, M. Sekiya, M. Hara, IEEE Trans. Electron Devices 42 (1995) 251.
- [5] A. Matsuda, J. Non-Cryst. Solids 59&60 (1983) 767.
- [6] Y. Chida, M. Kondo, A. Matsuda, J. Non-Cryst. Solids 198–200 (1996) 1121.
- [7] Y. Tsunoda, T. Sameshima, S. Higashi, Jpn. J. Appl. Phys. 39 (2000) 1656.
- [8] T. Sameshima, M. Satoh, Jpn. J. Appl. Phys. 36 (1997) 687.
- [9] K. Asada, K. Sakamoto, T. Watanabe, T. Sameshima, S. Higashi, Jpn. J. Appl. Phys. 39 (2000) 3883.